FORSCHUNGSZENTRUM
ROSSENDORF e.V.

FZR

FZR-103
September 1995
Preprint

H.-G. Ortlepp, W. Wagner, A.A. Aleksandrov, I.A. Aleksandrova, L. Dietterle, V.N. Doronin, S. Dshemuchadse, P. Gippner, C.-M. Herbach, D. Hilscher, S.I. Ivanovsky, A. Matthies, Yu.Ts. Oganessian, G. Pausch, Yu.E. Penionzhkevich, G. Renz, K.D. Schilling, D.I. Shishkin, O.V. Strekalovsky, V.V. Trofimov, C. Umlauf, D.V. Vakatov, V.M. Vasko, V.E. Zhuchko, A.G. Artukh, G.F. Gridnev, M. Grushezki, J. Szmider, Yu.G. Teterev, M.G. Nagaenko, Yu.M. Sereda, I.N. Vishnevski and S.G. Genchev

The COMBAS fragment separator of radioactive nuclei and the FOBOS 4π - detector for charged particles

Forschungszentrum Rossendorf e.V.
Postfach 51 01 19 · D-01314 Dresden
Bundesrepublik Deutschland

Telefon (0351) 260 3127
Telefax (0351) 260 3700
E-Mail schilling@fz-rossendorf.de

THE COMBAS FRAGMENT SEPARATOR OF RADIOACTIVE NUCLEI AND THE FOBOS [1] 4π - DETECTOR FOR CHARGED PARTICLES

H.-G. Ortlepp [2], W. Wagner [2],
A.A. Aleksandrov [3], I.A. Aleksandrova [3], L. Dietterle [2], V.N. Doronin [3],
S. Dshemuchadse [2], P. Gippner [2], C.-M. Herbach [2], D. Hilscher [4], S.I. Ivanovsky [3],
A. Matthies [2], Yu.Ts. Oganessian [3], G. Pausch [2], Yu.E. Penionzhkevich [3], G. Renz [2],
K. D. Schilling [2], D.I. Shishkin [3], O.V. Strekalovsky [3], V.V. Trofimov [3], C. Umlauf [2],
D.V. Vakatov [3], V.M. Vasko [3], V.E. Zhuchko [3], A. G. Artukh [3], G.F. Gridnev [3],
M. Grushezki [5], J. Szmider [5], Yu.G. Teterev [3], M.G. Nagaenko [8], Yu.M. Sereda [6],
I.N. Vishnevski [6], S.G. Genchev [7]

[2] *Research Center Rossendorf Inc., POBox 51 01 19, 01314 Dresden, Germany*
[3] *Joint Institute for Nuclear Research, 141980 Dubna (Moscow region), Russia*

ABSTRACT

The projectile-like fragment separator COMBAS is being designed at the Flerov Laboratory of Nuclear Reactions, JINR Dubna, for providing radioactive nuclear beams. COMBAS is a compact achromatic beam line with a high resolving power of 4360. It accepts fragments within 6.4 msr solid angle and with a momentum spread of 10%. The method of isotopic separation is based on a combination of magnetic rigidity and energy loss analysis. The separated radioactive beam is planned to be transported either into a time-projection chamber in the regime gas target - gas detector or to a secondary target positioned in the centre of the FOBOS 4π-array or to another set-up. The FOBOS detector is intended for heavy ion reaction studies in the bombarding energy range of 10-100 AMeV at the cyclotron U-400M of the FLNR. Presently, only primary cyclotron beams are used because COMBAS is not yet complete. FOBOS consists of a gas-detector ball of 30 position-sensitive avalanche counters and 30 axial ionization chambers behind them and an outer scintillator shell of 210 CsI(Tl) counters surrounding the gas detectors. An array of 96 phoswich counters covers the very forward angles. All charged reaction products can be measured in a wide dynamic range and in a geometry covering a substantial part of 4π. First data have been taken concerning fission and emission of intermediate-mass fragments in the reactions ^{7}Li (43 AMeV) on ^{232}Th and ^{14}N (34 AMeV) on ^{197}Au.

Contribution to the International Workshop on
" Physics with Recoil Separators and Detector Arrays "
New Delhi, India, January 30 - February 2, 1995

[1] The FOBOS project is supported by the BMBF, Germany, under contract Nr. 06 DR 671.
[4] Hahn-Meitner-Institute, Berlin, Germany.
[5] Henryk Niewodniczansky Institute for Nuclear Physics, Cracow, Poland.
[6] Institute for Nuclear Research, Kiev, Ukraine.
[7] Laboratory for Technical Developments, Bulgarian Academy of Sciences, Sofia, Bulgaria.
[8] D.V. Efremov Scientific Research Institute of Electrophysical Apparatus, St. Petersburg, Russia.

INTRODUCTION

After the reconstruction of the old U-300 heavy-ion cyclotron of the Flerov Laboratory of Nuclear Reactions into an isochroneous machine, the Fermi-energy range became available in the JINR Dubna. The new U-400M cyclotron is designed for beams up to 100 AMeV with intensities up to $> 10^{13}$ particles per second [1] . Due to its K-factor of about 400, the maximum specific energy of 100 AMeV can be reached only for ions with $q / A = 1 / 2$, i.e. for not too heavy ions. Such beams will be used mainly for the following research directions:

i) formation and decay of heavy hot nuclei with excitation energies of about 2-4 AMeV, i.e. in a transition region between "classic" reaction scenarios and multifragmentation
ii) nonequilibrium particle emission
iii) production of secondary radioactive beams with sufficient intensity for nuclear reaction studies

Because, on the other hand, beam energies near the Coulomb barrier will be possible at the U-400M too, typical low-energy phenomena may be traced to higher energies. The FOBOS array [2,3] is dedicated to studies according to (i), but may be also used for low-energy experiments. Its experimental programme has been started by the end of 1993 with fission investigations (see below). The COMBAS projectile-fragment separator [4] is presently being built up separately and after commissioning will be shifted to replace part of the presently existing beam-line from the U-400M to FOBOS. This unique combination should allow to perform nuclear reaction studies with high efficiency at radioactive beams.

DESIGN OF THE COMBAS FRAGMENT SEPARATOR

In peripheral heavy-ion induced nuclear processes at low and intermediate energies like transfer reactions, projectile fragmentation etc., broad element, mass, energy and angular distributions of the produced nuclei are realized. The large production cross sections of these projectile-like fragments and the possibility to use thick targets allow to achieve high production rates of nuclei far from the stability line. The large-acceptance fragment separator COMBAS is designed to select such nuclei with a high efficiency. Its doubly achromatic magnetic system [4] consists of a first analysing section and a second dispersion-compensating section , which are exactly mirror-symmetric with respect to the middle plane F_d of the system (fig.1). Each section is composed of two main bending analysing magnets (M_1 , M_2) and two auxiliary ones (M_3 , M_4). The focusing of the beam is achieved by alternative field gradients in M_1 and

M_2 , which focus the particles in the vertical and horizontal planes , respectively. The basic parameters of COMBAS are given in tab. 1.

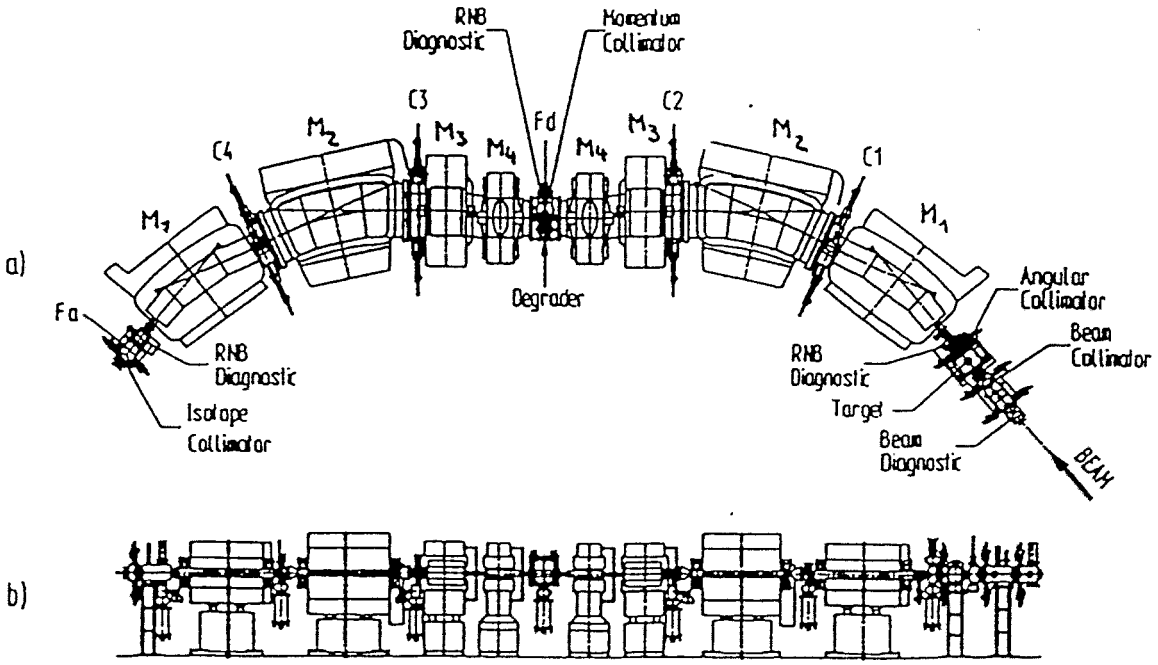

Fig. 1: Projectile-like fragment separator COMBAS (a: top view , b: side view).

A shaped degrader placed in the dispersive middle plane F_d allows to separate also different particles of the same magnetic rigidity.

Configuration	$\Delta\Omega$ (msr)	$\Delta p/p$ (%)	$B\rho$ (Tm)	$Rp/\Delta p$	L (m)
$M_1 M_2 M_3 M_4 F_d M_4 M_3 M_2 M_1$	6.4	± 10	4.5	4360	14.5

Tab. 1: Basic parameters of COMBAS.

THE 4π-DETECTOR ARRAY FOBOS

The main task of FOBOS is to identify as many as possible charged particles from multiple events and to determine their velocity vectors. A multi-detector principle was chosen with such detector cells, which can handle only one particle of a certain multiple event. As it is impossible to cover the whole dynamic range expected for the particle masses and kinetic energies by use of only one shell of counters of a certain type, different detector types have been combined.

The granularity is determined by the expected multiplicities. 30 position-sensitive avalanche counters (PSAC) and 30 axial ("Bragg") ionization chambers (BIC) will detect 2-6 heavy and intermediate-mass fragments (IMF). In order to stop penetrating light charged particles (LCP), 210 scintillation counters are placed behind the BIC s [2] .

All detectors are arranged in 30 modules placed on the facets of a polyeder (12 regular pentagons and 20 regular hexagons). Two pentagons are used for the beam entry and exit (fig.2).

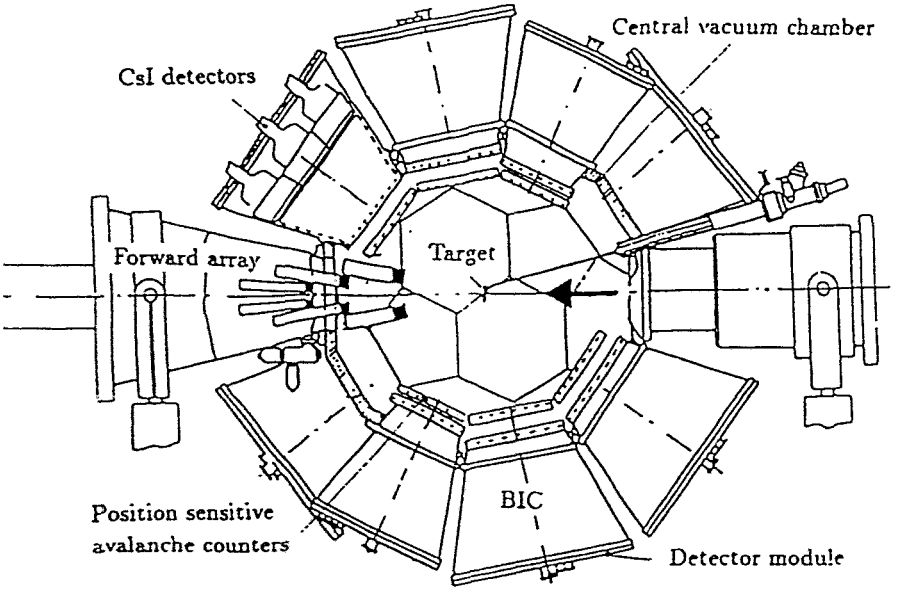

Fig. 2: Cut of the FOBOS detector.

The physical quantities of the detected particles are derived from the counter signals as shown in fig. 3. The flight path (target - PSAC) amounts to 50 cm and the depth of the BIC to 25 cm. For projectile-like fragments and preequilibrium particles emitted under very forward angles ($\vartheta < 25°$), an array of 92 plastic+BGO phoswich counters is being installed [5].

All detector modules are held in their position by a central support frame acting also as vacuum chamber (fig. 2). Every counter gas-volume is connected through two valves with collector rings, through which evacuation and gas supply is performed. To compensate the gas deterioration, a pressure-stabilized flow-through regime is utilized. The pressure ranges amount to 200-800 Pa of pentane for the PSACs and to 10-100 kPa of P10 (90% Ar + 10% methane) for the BICs. All components can be controlled either manually or remotely by a SIEMENS SX automation system. The actual pressure values can be observed at 64 different positions of the system.

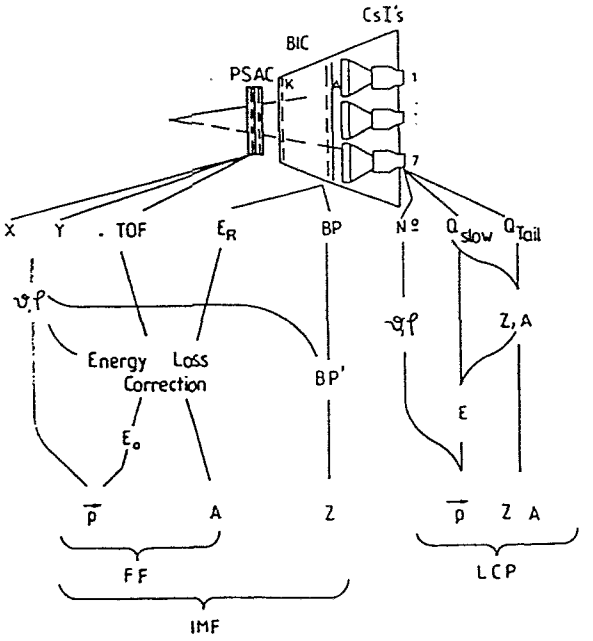

Fig. 3: Derivation of measured quantities from the detector signals

The PSACs are based on the principles described in ref. [6]. A central cathode foil delivers the timing signal and two anode wire planes serve as coordinate grids. Three 120 $\mu g/cm^2$ polyester foils are utilized. The outer ones act as windows and the central one coated with 40 $\mu g/cm^2$ gold layers on both sides as cathode. The counter frames have pentagonal and hexagonal shapes on their periphery and circular apertures of diameter 243 mm and 327 mm, respectively, as sensitive areas. The sensitive gaps amount to 3 mm. W-wires (goldplated, 30 µm diameter) spaced by 1 mm serve as anode. Every two neighbouring wires are connected with one conductive strip and capacitively coupled to a delay line.

The BICs are cones with 27.6° and 34.8° opening angles and entrance window diameters of 285 mm and 385 mm, respectively . The window foils are supported by a twofold structure:

A heavy carrier of 94 % transparency and an etched nickel mesh with 2.7 mm cells of 66 % transparency. The field shaping is performed by copper strips providing equal potential steps, i.e. a homogeneous field. The Frisch grid consists of two perpendicular planes of 1 mm spaced 50 µm Cu-Be wires. The anode placed 10 mm behind the Frisch grid is made of 10 µm thick aluminized MYLAR and is penetrated by light charged particles to be detected in the scintillation counters.

The electron drift time of up to 4 µs would cause a large ballistic deficit in the case of conventional pulse shaping. Therefore, a digital processing method [7] is utilized, which derives the energy and Bragg-peak height from digitized signal samples (fig. 4).

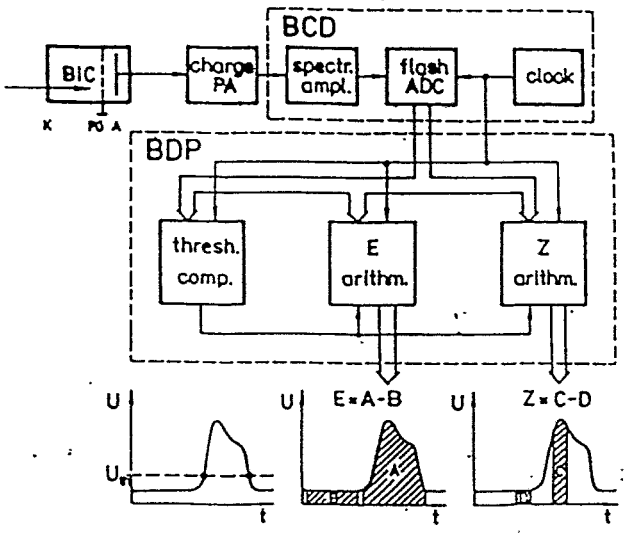

Fig. 4: Principle of the new signal processing method for Bragg-peak spectroscopy.

The PSACs and BICs are not capable of detecting low-ionizing high-energetic light charged particles. Therefore, a shell of 210 CsI(Tl) counters is arranged behind the gas detectors [8]. The scintillators are hexagonal shaped crystals (∅ 200 mm and ∅ 150 mm, respectively) covering the sensitive area of the BIC with a geometrical efficiency of 73.4 %. Seven crystals are joined in each module. The scintillators have thicknesses of 1.5 cm and 1 cm for laboratory angles of $\vartheta \approx 16°\text{-}52°$ and $\vartheta \approx 53°\text{-}164°$, respectively, to stop LCP up to 50-63 AMeV. For alpha particles of ^{238}Pu, typical resolutions of the scintillation detectors of 6-7 % have been achieved. LCP are discriminated up to Z = 3 applying a pulse-shape analysis method [9].

The front-end electronics of one gas-detector module occupy 5 CAMAC stations and deliver 5 parameters: The Bragg-peak height and the energy derived from the BIC as well as two co-ordinates and the time-of-flight (TOF) from the PSAC. The signals of the scintillation counters are split and digitized within two gates by use of FASTBUS charge digitizers. The cyclotron RF- signal serves as a time reference . In the first experiments, the delayed "start"-signals of two small transmission counters positioned near the target had to be used. The whole gas-detector electronics occupy 9 CAMAC crates connected via VDBbus with an EUROCOM-6 VME work station. The FASTBUS crate is included into the VDB branch. The software for CAMAC access and data transfer from the VME station via Ethernet to a SUN computer has been developed and implemented into the HOOPSY data acquisition system [10].

The mass determination for the particles stopped in the BIC is based on the TOF, kinetic energy and emission angle measured (fig. 3). The energy loss the particle suffers in the PSAC before reaching the BIC is taken into account. For this purpose, an iterative procedure [3] has been developed , which reproduces the initial energy and the mass of the particle. The known mass distributions of ^{244}Cm (sf) and ^{252}Cf (sf) measured in several test runs could be well reproduced.

FIRST EXPERIMENTS WITH FOBOS

In order to investigate fission after incomplete fusion accompanied by the emission of LCP and IMF at excitation energies of up to about 300 MeV, we used the reaction ^{7}Li (43 AMeV) + ^{232}Th [11]. A 270 $\mu g/cm^2$ thick ^{232}Th-layer was deposited on a 50 $\mu g/cm^2$ thick Al_2O_3 backing.

Ten PSACs, 12 BICs and 10 CsI(Tl) counters were operated in the first runs. The geometrical arrangement of the modules has been chosen according to Monte-Carlo simulations of triple events including possible neck emission of IMF. The entire expected range for the folding angle of the fission fragments (FF) was covered by respective detector-module pairs. In this arrangement, all the other modules but those detecting the two FF could record the IMF.

Two transmission avalanche counters were placed near the target in direction of two modules at ϑ=37° to deliver the needed "start"-signals. Any fragment recorded in one of the "start"-counters could trigger the data acquisition system. The event was stored, if one or more additional PSACs fired within a timing interval of 200 ns.

The BICs and PSACs were operated in a gas flow-through regime at pressures of 26 kPa of P10 gas mixture and 530 Pa pentane, respectively. The PSAC bias was set at a value about 5 Volts below the onset of spark discharges what guaranteed an efficient detection of fragments from FF down to alpha particles.

Up to now, $3.1 \cdot 10^6$ events with at least two recorded FF have been scanned for IMF-FF-FF coincidences. The FF were identified by gates set in the TOF-TOF-distributions, the IMF (for $3 \leq Z \leq 8$; $E > 1.2$ AMeV) by gates both in the respective TOF-E and Z-E distributions. Thus, 230 triple events were obtained altogether for the various module combinations and with additionally restricting the IMF emission angles to $\vartheta > 80°$ in the laboratory system, where the equilibrium component dominates.

As a first result, the yields of IMF-accompanied fission relative to binary fission have been determined in dependence on the excitation energy (E*) , which was assumed to be proportional to the linear momentum transfer (LTM), and the angle $\Theta_{IMF\text{-}FF}$ between the fission-axis and the direction of the IMF- emission. The few events available up to now allow only a rough division into few intervals in E* and $\Theta_{IMF\text{-}FF}$.

On the condition that two FF were measured in coincidence by module (i) and module (j), the geometrical acceptance ε (i, j, k) for the detection of a third particle by module (k) strongly depends on the center-of-mass velocity $v_{c.m.}$ of the composite system. The longitudinal component of $v_{c.m.}$ corresponds with the momentum tranferred from the projectile to the target nucleus by incomplete fusion. In particular for central collisions, the transversal $v_{c.m.}$-component results from evaporated neutrons and LCP emitted at the de-excitation cascade before fission. Certainly, the momentum balance of the ternary decay itself has also to be taken into account.

Within the frame of the following assumptions, the geometrical efficiencies ε (i, j, k) have been estimated by Monte-Carlo simulation:

i) The mean velocity of the fissioning system in beam direction was obtained for each of the module pairs (i, j) from the experimental fission fragment folding angle distribution.

ii) The angular distribution of the transversal $v_{c.m.}$-component was generated by isotropic neutron emission. In order to verify this procedure, the coplanarity distribution ($\Phi_i - \Phi_j$) was analysed, which is a good observable to scale the transverse $v_{c.m.}$-component. By optimizing the assumed number of emitted neutrons M_n , a close agreement between the calculated and the measured coplanarity distributions was achieved. The expected relation $M_n - E^*$ was reproduced for different fission detector pairs.

iii) Within the limited solid angles that are covered by the different module pairs, the fission yield was approximated to be isotropic. The fragment mass distribution was assumed to be Gaussian-like, the kinetic fragment energies correspond with the VIOLA-systematics.

iv) The deduced ε (i, j, k)-values applied in eq. (1) are calculated under the assumption of isotropic IMF-emission with the mean kinetic energy of 4 AMeV

v) The solid supporting grid in front of the entrance window of the BIC caused a transparency of only 60% for the IMF-detection.

With N_{IMF} (i, j, k) triple and N_{FF} (i, j) binary events for a certain module combination (i, j, k), the measured IMF-yield (into 4π) per fission is expressed by eq. (1):

$$Y_{ijk} = N_{IMF}(i, j, k) / (N_{FF}(i, j) \cdot \varepsilon_{ijk}) \qquad (1)$$

These yields have been selected into a low-LMT group ($\Delta p \approx 50\%$, $E^* \approx 150$ MeV) and a high-LMT group ($\Delta p \approx 80\%$, $E^* \approx 230$ MeV). The yields for five mean angles $\Theta_{IMF\text{-}FF}$ are shown in fig. 5.

The Y_{ijk} for low LMT show no significant variation with $\Theta_{IMF\text{-}FF}$ between 35° and 90°. The mean value of this IMF-component amounts to $(0.7 \pm 0.1) \cdot 10^{-3}$ IMF-accompanied fissions per binary fission. For the higher LMT , this value increases to $(2.3 \pm 0.3) \cdot 10^{-3}$.

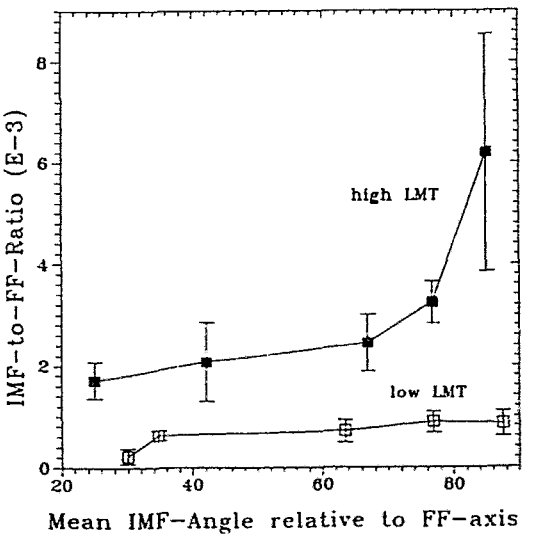

Fig. 5: Yields Y_{ijk} for certain mean angles Θ_{ijk} according to low LMT (open squares) and high LMT (full squares)

Recently, IMF-yields per nuclear reaction have been reported in ref. [12]. There, E* has been determined by the multiplicity of evaporated neutrons. The experimental IMF-energy spectra measured at backward angles could be interpreted assuming an equilibrated target-like source. Our measuring conditions, i.e. a very light projectile and the IMF-detection at backward angles, give special sensitivity to such a source. Therefore, we compared our yields with the data of ref. [12] in the adequate range of E*, that is, for neutron multiplicities of 10-20. Such a comparison gives the same trend of an increasing yield with E*, but our IMF-yields per fission are lower by more than one order of magnitude compared to the value evaluated from ref. [12] : $\approx 3 \cdot 10^{-2}$ fragments with Z = 3 per reaction into 4π. This means that fission after an IMF-emission is highly suppressed and the production of heavy residues becomes more probable.

The enhanced IMF-yield near $\Theta_{IMF\text{-}FF} = 90°$ for higher E* confirms the existence of a further source, the strength of which also increases with E*. Possibly, these IMF are emitted from the neck-region of the fissioning system at scission as claimed in ref. [13]. If we consider $\Theta_{IMF\text{-}FF}$ within an interval of $90° \pm 10°$ relative to the fission axis (fig. 5), a rough estimate of the probability for neck-emission of IMF results in a value of several units times 10^{-4} per binary fission. It is by about one order of magnitude higher than in the case of low-energy (spontaneous or thermal neutron induced) ternary fission [14]. Any attempt to explain this drastic increase by considering the excitation energy remaining in the system at the scission point [15] and a temperature-dependent probability for neck-particle emission has failed so far.

The investigation of binary and ternary decay of hot heavy nuclei has been continued using the reaction ^{14}N (34 AMeV) + ^{197}Au. The target was a 500 $\mu g/cm^2$ thick gold foil. 16 gas-filled detector modules and 80 CsI(Tl)-counters were operated. One of the two "start"-counters remained at the forward angle ϑ=37°, but the second one has been positioned at ϑ=101° relative to the beam axis to trigger on backward-emitted fragments.

In addition, the PSAC pulse height (ΔE) of the fragments was measured. By this way, using the ΔE- and TOF-information delivered by the PSAC, it was possible to roughly identify also slow particles , which did not enter the BIC.

About $2.5 \cdot 10^6$ events with two and $2 \cdot 10^3$ events with three fragments hitting the gas modules have been recorded. A first estimate of the ratio of triple (FF+FF+IMF) to binary (FF+FF) decays for events with LMT ≈ 80% yields a value of about $2.5 \cdot 10^{-3}$. This value is comparable with that obtained for the former reaction ^{7}Li + ^{232}Th. The larger statistics in the present experiment, however, should allow a more detailed analysis.

The CsI(Tl)-detectors recorded one additional LCP in about 50 % of the events.

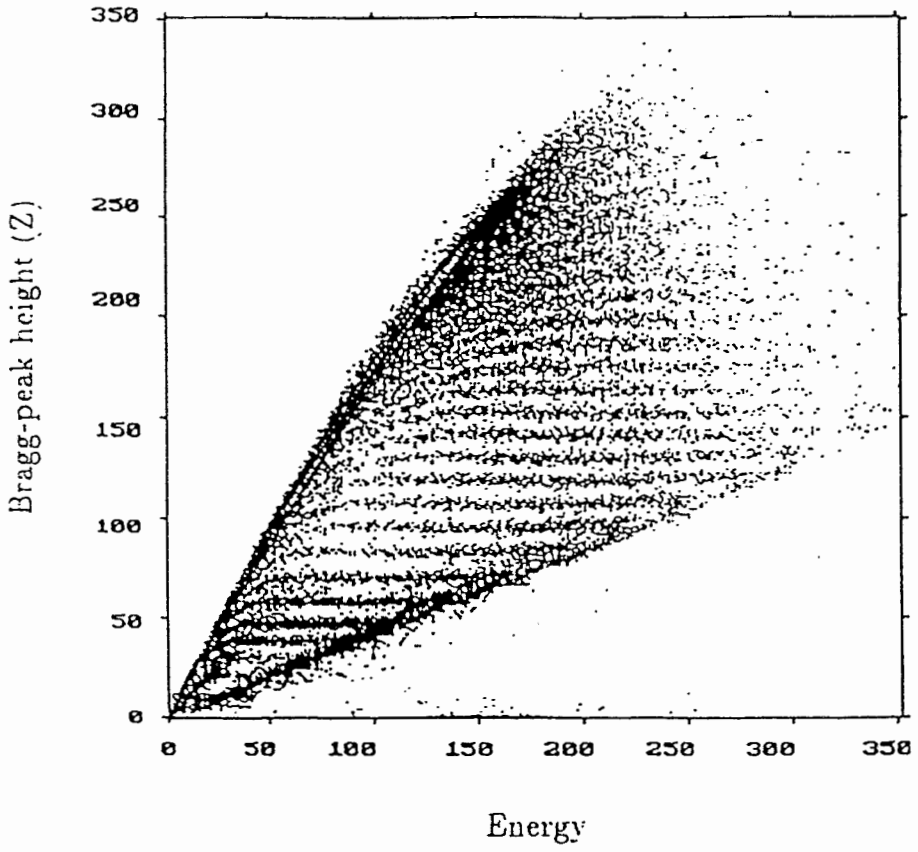

Fig. 6: Bragg-peak height vs. energy plot of particles recorded by a BIC at 37°. Z-branches from 2 to 25 are resolved. The transition to unresolved FFs is smooth.

A first scan of the data shows some interesting features to be analyzed :

i) There is a smooth transition from symmetric to very asymmetric fission ($A_1/A_2 \approx 10$) both in the yield and in the fragment energy (fig.6).

ii) Coincident with a sideward-emitted light fragment (IMF), either a heavy residue or fission fragments are observed (fig.7).

iii) Both in symmetric and asymmetric fission, there is a considerable probability of LCP-emission into backward directions.

From the further analysis now in progress, new information about the competition between binary and ternary decay of hot nuclei with mass numbers $A \approx 190$ and excitation energies of $E^* \approx 300$ MeV as well as the probability for survival of a heavy residue are expected.

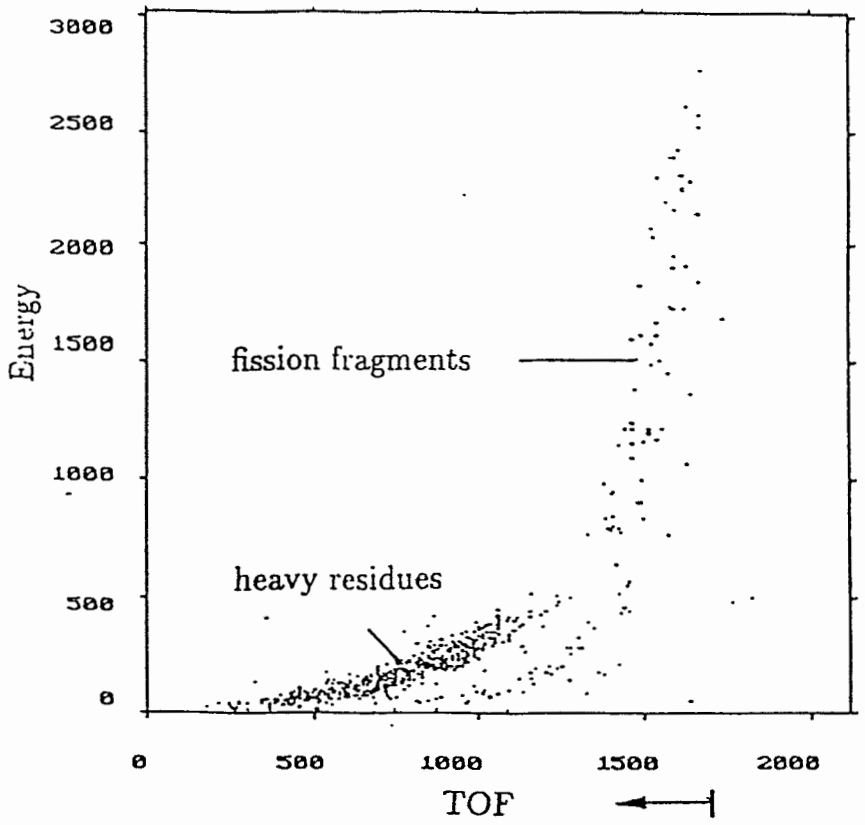

Fig. 7: Energy vs. TOF plot of a module at ϑ=37°. Only events in coincidence with IMF emitted under ϑ=101° were selected. The two distinct groups can be interpreted as the heavy partners of a binary process and as fragments of their subsequent fission.

REFERENCES

[1] Yu. Ts. Oganessian et al., Proc. Int. Conf. on Exotic Nuclei, Foros, Crimea, Ukraine (1991): Ed.Yu.E. Penionzhkevich, R. Kalpakchieva (World Scientific, Singapore, 1992) p.3

[2] H.-G. Ortlepp et al., Proc. Int. Conf. on New Nuclear Physics with Advanced Techniques, Ierapetra, Crete, Greece (1991): Ed. F.A. Beck, S. Kossionides, C.A.Kalfas (World Scientific , Singapore, 1992) p.302

[3] H.-G. Ortlepp et al., Proc. Int. School-Seminar on Heavy Ion Physics, Dubna, Russia, (1993): Ed. Yu.Ts. Oganessian, Yu.E. Penionzhkevich, R. Kalpakchieva (JINR Dubna, 1993) vol.2 , p.466

[4] A.G. Artukh et al., Nucl. Instr. and Meth. in Phys. Res. A306 (1991) 123

[5] W. Terlau et al., Annual Report 1989 (HMI Berlin, Germany) HMI-482 (1990) 93

[6] W. Seidel et al., Nucl. Instr. and Meth. in Phys. Res. A273 (1988) 536

[7] H.-G. Ortlepp and A. Romaguera, Nucl. Instr. and Meth. in Phys. Res. A276 (1989) 500

[8] W. Wagner et al., Scientific Report 1991 - 1992 (FLNR, JINR Dubna) E7-93-57 (1993) 244

[9] J. Alarja et al., Nucl. Instr. and Meth. in Phys. Res. A242 (1986) 352

[10] G. Röschert et al., Report HMI - 436 (1986) Hahn-Meitner-Institut Berlin, Germany

[11] A.A. Aleksandrov et al., Proc. 5th Int. Conf. on Nucleus-Nucleus Collisions, Taormina, Italy (1994): Nucl. Phys. A583 (1995) 465

[12] A. Sokolov et al., Nucl. Phys. A562 (1993) 273

[13] D.E. Fields et al., Phys. Rev. Lett. 69 (1992) 3713

[14] Theobald et al., Nucl. Phys. A502 (1989) 343c

[15] Hilscher and H. Rossner, Ann. Phys. Fr. 17 (1992) 471